



A novel method for acquiring rigorous temperature response functions for electricity demand at a regional scale

Yuki Hiruta ^{*}, Lu Gao, Shuichi Ashina

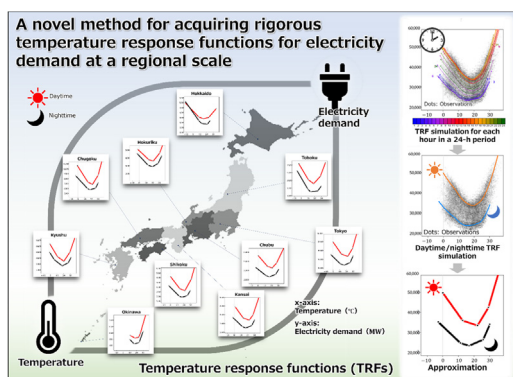
Social Systems Division, National Institute for Environmental Studies, 16-2 Onogawa, Tsukuba, Ibaraki 305-8506, Japan



HIGHLIGHTS

- Rigorous temperature response functions (TRFs) were acquired at a regional scale.
- The MARS algorithm was used to model demand for electricity.
- TRFs for each hour in a 24-h period were quantified in simulations using MARS.
- Temporal segments in TRFs were identified and should be considered in future work.
- Reliable TRFs and parameters for approximated simple functions are provided.

GRAPHICAL ABSTRACT



ARTICLE INFO

Article history:

Received 26 February 2021

Received in revised form 17 October 2021

Accepted 30 December 2021

Available online 4 January 2022

Editor: Martin Drews

Keywords:

Temperature response function

Electricity demand

Temperature

Human activities

Multivariate adaptive regression splines (MARS)

Climate change

ABSTRACT

The demand for electricity affects the future climate through its effect on greenhouse gas emissions in the electricity generation process, but climate change also impacts electricity demand by changing the need for heating and cooling. Developing reliable temperature response functions (TRFs) that illustrate electricity demand as a function of temperature is key for decreasing uncertainty in future climate projections under a changing climate and for impact assessments of climate change on energy systems. However, this task is challenging because electricity demand is determined by multiple factors that interact in complicated ways because demand fluctuations represent timely human responses to given meteorological conditions. We propose a novel method to acquire reliable TRFs at a regional scale based on comprehensive modeling of electricity demand fluctuations. Six candidate algorithms were examined, and multivariate adaptive regression splines (MARS) was selected as the best algorithm with the dataset used. Using MARS, we constructed models with the capacity to precisely reproduce complex electricity demand patterns based on multiple predictors and simulated the impact of temperature on electricity demand while controlling for the effects of other factors. The temporal segments in TRFs are detected and parameters and functional forms of TRFs for 10 regions in Japan were presented.

1. Introduction

Electricity demand affects the future climate through greenhouse gas emissions in the energy generation process, but climate change also impacts

energy demand by changing the needs for heating and cooling (Mideksa and Kallbekken, 2010; Schaeffer et al., 2012; Aufhammer and Mansur, 2014; Emadi et al., 2019; Yalew et al., 2020). In such complicated feedback loops, uncertainties abound in both energy demand estimates and climate change projections. Because the ambient temperature is affected by the global and local climate, urban heat islands (UHIs) also affect energy demand in urban areas (Hirano and Fujita, 2012; X. Li et al., 2019). There may be a positive feedback loop between waste

^{*} Corresponding author.

E-mail addresses: hiruta.yuki@nies.go.jp (Y. Hiruta), gao.lu@nies.go.jp (L. Gao), ashina.shuichi@nies.go.jp (S. Ashina).

Glossary¹

UHI	urban heat island
HDD	heating degree days
CDD	cooling degree days
TRF	temperature response function ²⁴
BPT	balance point temperature
BPE	balance point electricity demand
MARS	multivariate adaptive regression splines
RF	random forest
SVR	support vector regression
ANN	artificial neural network
GAM	generalized additive model
OLS	ordinary least squares (for linear regression model)
GCV	generalized cross validation
MAPE	mean absolute percentage error
RMSPE	mean absolute percentage error
VI	variable-importance measure

¹ See Table 1 for the abbreviations of variable names.

heat from air conditioning and increased demand for air conditioning, but it is not well understood. Increasing temperatures are expected to significantly impact the power sector because there is no alternative for cooling (Dirks et al., 2015; Wang and Bielicki, 2018; Moazami et al., 2019; Morakinyo et al., 2019). The relationships between meteorological conditions and electricity demand on a regional scale must be clarified to understand such complex mechanisms. Therefore, to help strengthen the scientific basis for managing electricity systems efficiently, to assess the impacts of UHIs and extreme weather events caused by climate change, and to derive reliable mitigation and adaptation measures against the warming environment, a method for acquiring rigorous temperature response functions (TRFs) of electricity demand should be developed.

Because temperature is the most important meteorological determinant of electricity demand (e.g., Yildiz et al., 2017), TRFs (also referred to as dose-response functions, temperature-energy demand functions, and energy signatures) are often used to project electricity consumption under different climate change scenarios (Franco and Sanstad, 2008; Auffhammer and Aroonruengsawat, 2011; Auffhammer and Mansur, 2014; Allen et al., 2016; Auffhammer et al., 2017; Wenz et al., 2017; Y. Li et al., 2019).

TRFs are also used to determine the balance point temperature (BPT) (Woods and Fuller, 2014; Krese et al., 2018), which represents the temperature at the bottom of a V-shaped TRF (Amato et al., 2005; Ruth and Lin, 2006) (Fig. 1). The BPT is used as a reference temperature to derive heating degree days (HDD) and cooling degree days (CDD) (Lindelöf, 2017), which is the number of degrees that the average temperature during a given period is below (or above) a certain temperature. A number of studies rely on HDD/CDD to predict future electricity demand (e.g., Matzarakis and Balafoutis, 2004; Christenson et al., 2006).

Although many studies have determined TRFs for single buildings (e.g. Lindelöf, 2017; Verbai et al., 2017), TRFs at city, regional, national, and global scales are not well established. In reality, there is no established method to determine regional and temporal variations in relevant parameters, such as regression coefficients or BPTs in TRFs (Fazeli et al., 2016). Therefore, many studies have had no alternative but to apply BPTs defined by expert institutions in individual countries (e.g., Asai et al., 1999; Nitta et al., 2005; Trust, 2012; ASHRAE, 2013; CIBSE, 2006; Krese et al., 2018). Such uncertainty regarding the choice of TRFs may increase the risk of incorrect estimates in studies that provide a basis for policymaking or propose strategies to improve energy

efficiency and measures against climate change (Woods and Fuller, 2014; Lindelöf, 2017).

In this study, the electricity demand at the BPT in a V-shaped TRF is denoted as the “balance point electricity demand” (BPE), while the flat section between the heating and cooling demand slopes in a U-shaped TRF is defined as the “comfort zone” (Brown et al., 2016; Fazeli et al., 2016; Wang and Bielicki, 2018) (Fig. 1).

Higher ambient temperatures decrease the heating demand in the cold season and increase the cooling demand, thus amplifying peak loads, in the hot season (Segal et al., 1992; Ruth and Lin, 2006; Hamlet et al., 2010; De Cian et al., 2013; Braun et al., 2014; Zhou et al., 2014; Wang and Chen, 2014; Auffhammer and Mansur, 2014; Invidiata and Ghisi, 2016; Auffhammer et al., 2017; Wenz et al., 2017; Y. Li et al., 2019). Previous studies have proposed numerous methods to identify the nonlinear relationships between temperature and electricity demand. A number of studies have divided observations by season or time and applied the ordinary least squares (OLS) method to obtain partial TRFs by season and time (e.g., Kittaka and Miyazaki, 2014; Hirano et al., 2017; Kiyokawa and Narumi, 2018). In some studies, the influence of confounders in the observations was corrected based on the estimated parameters obtained by multiple linear regression models, and the percentiles (e.g., the median) of the observations for each temperature bin were then linked to represent the flexible relation between the temperature and electricity demand (e.g., Auffhammer and Aroonruengsawat, 2011; Auffhammer et al., 2017; Wenz et al., 2017). Statistical models, such as the spline function (Y. Li et al., 2019), segmented regression technique (Ihara et al., 2008; Wang and Bielicki, 2018; Hashimoto et al., 2019), logistic smooth transition method (Moral-Carcedo and Pérez-García, 2015), and panel threshold regression (Bessec and Fouquau, 2008), have been applied to identify nonlinearities between variables. Studies that apply statistical algorithms have recently become more prevalent, for example, the artificial neural network (ANN; Beccali et al., 2008), random forest (RF; Mukherjee and Nateggi, 2017, 2019), multivariate adaptive regression splines (MARS; Sigaue and Chikobvu, 2010; Mukherjee and Nateggi, 2017, 2019; Al-Musaylh et al., 2018), Bayesian additive regression trees (Nateggi and Mukherjee, 2017; Mukherjee and Nateggi, 2017, 2019; Mukherjee et al., 2019), support vector regression (SVR; Al-Musaylh et al., 2018), autoregressive integrated moving average (Al-Musaylh et al., 2018), and Gaussian mixture model regression (Wang et al., 2018). However, there is no established method for estimating TRF (Lindelöf, 2017).

Several studies have reported the effects of multiple meteorological factors other than temperature on electricity demand, such as humidity (Sailor and Muñoz, 1997; Ihara et al., 2008; Auffhammer and Mansur, 2014; Amber et al., 2015; Wang and Bielicki, 2018; Y. Li et al., 2019; Hashimoto et al., 2019; Hiruta et al., 2019; Maia-Silva et al., 2020). However, few studies have generated TRFs considering the influence of factors other than temperature.

In addition, most studies have used daily, monthly, or yearly aggregated electricity consumption data (e.g., Auffhammer and Aroonruengsawat, 2011; Auffhammer et al., 2017; Wenz et al., 2017; Wang and Bielicki, 2018) without examining the temporal differences in the reported TRFs (Wang and Bielicki, 2018; Kiyokawa and Narumi, 2018; Hiruta et al., 2019). At such aggregated time resolutions, the intensive impacts that occur at diurnal and seasonal peaks and the impacts caused by certain combinations of factors cannot be detected. Detecting such simultaneous interactions become increasingly important as the frequency and intensity of extreme meteorological events are expected to increase due to climate change (Fischer and Knutti, 2015).

We propose a methodology based on three basic ideas: 1) the mechanisms through which fluctuations of electricity demand are determined should be comprehensively modeled by considering the effects not only of temperature but also of other factors; 2) the time boundaries in the relationship between temperature and electricity demand

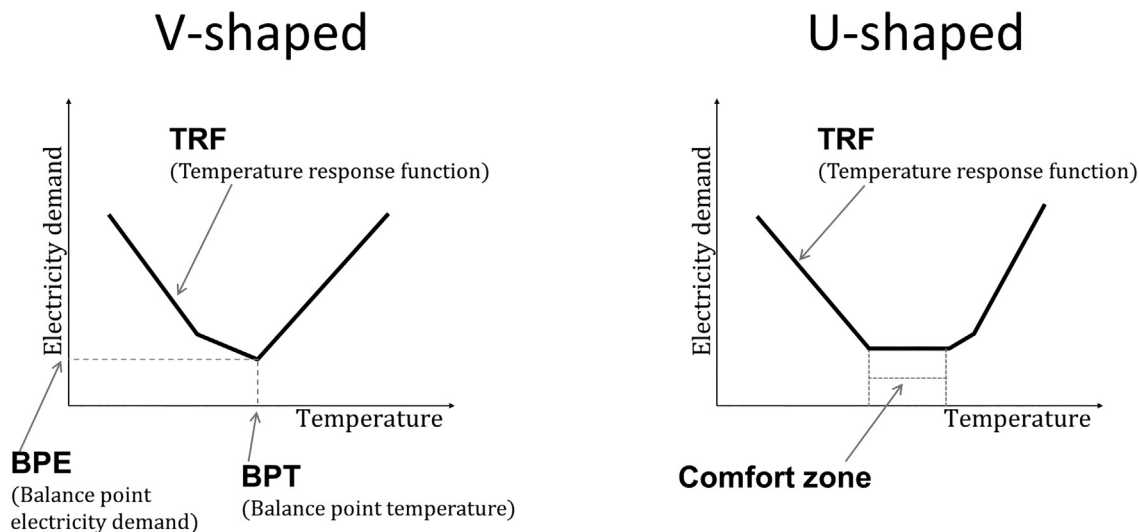


Fig. 1. Illustrated concepts of TRF, BPT, BPE, and comfort zone.

should be detected for providing rigorous TRFs that represent each region; and 3) the simulations to generate TRFs should be conducted controlling the effect of factors other than the temperature. To the best of our knowledge, no previous study has determined TRFs through simulations using these three concepts as a basis. The challenge is to construct comprehensive models of high enough quality to repeatedly reproduce the sensitivity of electricity demand to temperature under specified conditions, not merely to build models with high predictive performance.

Our aim was to propose a series of novel methods to acquire reliable TRFs at a regional scale that can contribute to assessing the impacts of future climate change on electricity demand as well as to the efficient management of electricity systems. The proposed methodology is based on simulations using precise regression models that have the capacity to reproduce fluctuations in electricity demand based on multiple predictors. Fig. 2 illustrates the framework of this study.

The variables, data sources, study area, and study period for the dataset are described in Section 2, and algorithm selection is explained in Section 3. In Section 4, regression models are constructed for each region, and model performances are rigorously examined in terms of the accuracy of prediction, generalization ability, year dependency, and the reasonability of the contribution of each predictor. Simulations are conducted in Section 5 to determine TRFs while keeping variables fixed to control for the effect of factors other than temperature. The hourly TRFs are simulated to investigate whether there are distinct segments among the 24 hourly TRFs; seasonal differences in TRFs are also examined. Finally, precise TRFs and approximated simple TRFs and their parameters are provided. Section 6 summarizes the results and offers conclusions.

2. Datasets

2.1. Study areas

The study areas were the jurisdictions of the 10 major electricity companies (EPCs) from Hokkaido to Okinawa in Japan (Fig. 3). The location of the most populated city in each jurisdiction ranges from 43°04'N (Sapporo, Hokkaido) to 26°12'N (Naha, Okinawa).

2.2. Study period

The target period ranged from 1 April 2016 to 31 March 2019, which corresponds to the 2016, 2017, and 2018 fiscal years in Japan.

We selected this period because hourly electricity demand data before April 2016 are not available, and we wanted to avoid the impact of COVID-19 on electricity demand in and after 2020.

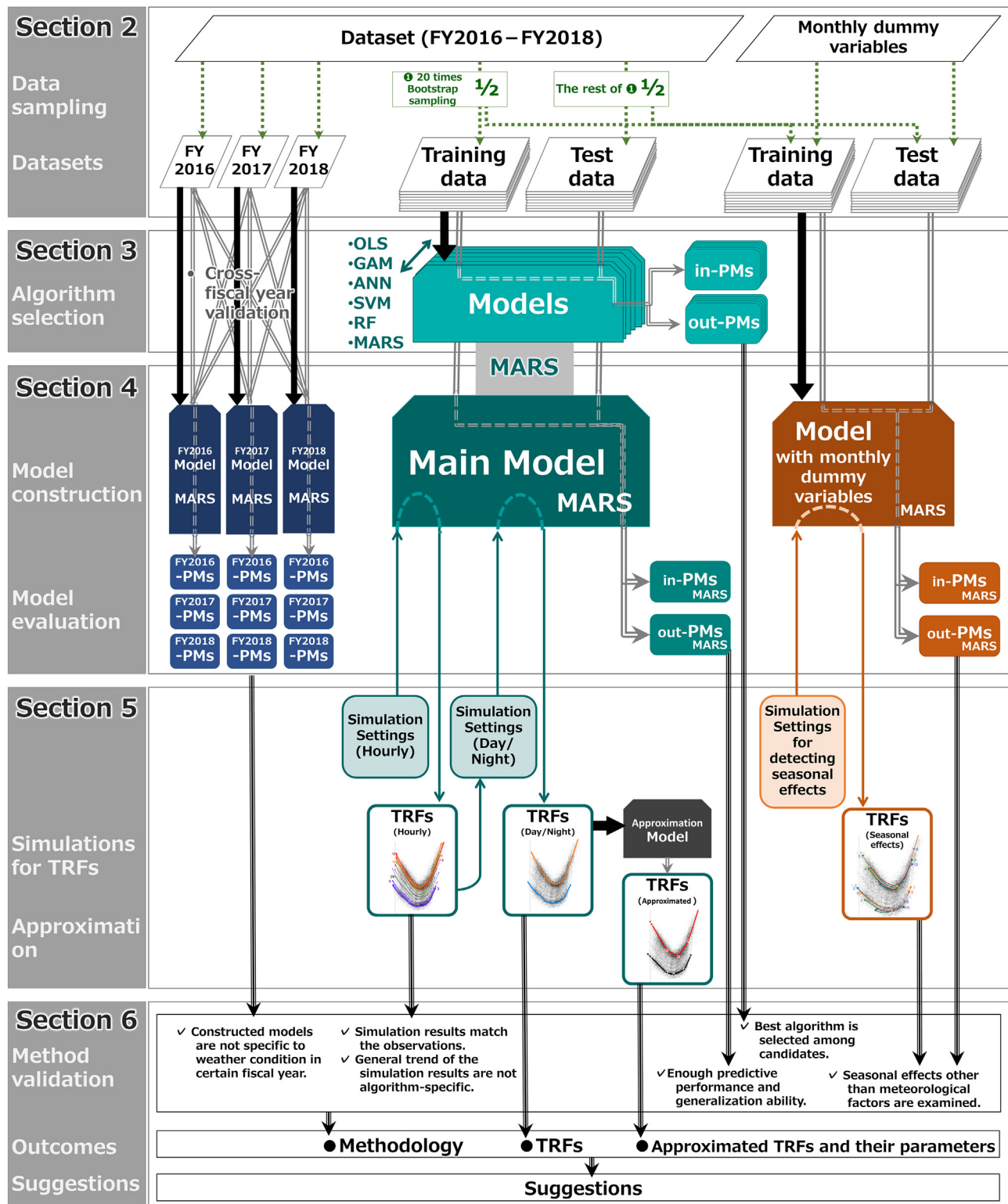
2.3. Variables and the data sources

Table 1 summarizes the candidate variables and data sources. The objective variable is the hourly power demand data (Organization for Cross-regional Coordination of Transmission Operators, 2020) recorded during the target period in each of the 10 regions.

Eighteen predictors were applied as the candidate explanatory variable. Seven types of hourly historical weather data (Japan Meteorological Agency, 2020), which are observed at weather stations in the most populated cities in each region, were used as the meteorological indicators: temperature (TEMP); humidity (HUM); wind speed (WIND); solar radiation (SUN); rainfall (RAIN); snowfall (SNOW1); and snow depth (SNOW2). The thermal indices generated from meteorological indicators—discomfort index (DI), wind chill index (WCI), and dew point temperature (DPT)—were also adopted because they might explain electricity demand induced by human reactions to a given thermal environment better than the simple application of the meteorological factors. The data and variables are described in more detail in Appendices A–C.

Four dummy variables for Sundays and holidays (SunD), Saturdays (SatD), consecutive holidays (ConD), and non-working days (NwdD) were applied to distinguish day types. Time usage surveillance data (NHK Broadcasting Culture Research Institute, 2015) were applied to consider the influence of the daily routine of human activities, namely, the percentage of the population in a given hour that is working (WORK%), asleep (SLEEP%), in their homes (HOME%), and awake in their homes (AWAKE%). Different time usage surveillance data were applied for weekdays, Saturdays, and Sundays and holidays, but not according to region or fiscal year.

Most of the indicators that have been used as predictors of electricity demand in past studies were considered as candidates. However, indicators with coarse temporal resolution could not be incorporated because they cannot explain the dispersion in hourly electricity demand in each region. For example, data on socioeconomic factors (e.g., population and gross domestic product) and CDD/HDD are released annually or even less frequently, which is clearly too coarse to explain the dispersion of hourly electricity demand during the study period (FY2016–FY2018). The spatial variation of these indicators is also not available,



* in-PMs and out-PMs denote the performance metrics based on the evaluation using the in-sample (training) data and out-of-sample (test) data, respectively.

* FY2016-PMs, FY2017-PMs, and FY2018-PMs denote the performance metrics based on the evaluation using the data observed in FY2016, FY2017, and FY2018, respectively.

Fig. 2. Overview of the study framework.

meaning that only a single observation is available in each region. The impacts of such region-specific socioeconomic factors are, however, incorporated into the models as parameters estimated in the development of each model.

3. Algorithm selection

The performance of the six candidate algorithms was evaluated based on three performance metrics for in-sample/out-of-sample results

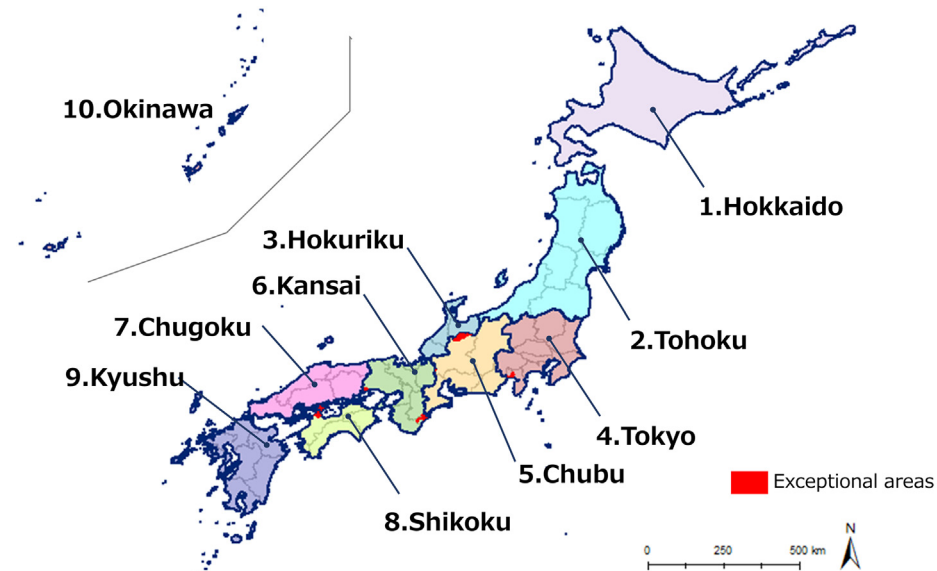


Fig. 3. Study areas (colors denote the jurisdictions of electricity providers).

(i.e., the results based on the datasets that were used/not used for model training). The algorithm that performed best with the datasets applied was selected.

3.1. Candidate algorithms

The candidate algorithms were OLS, a generalized additive model (GAM), support-vector regression (SVR), ANN, RF, and MARS. The details of the algorithms are summarized in Table 2.

3.2. Performance evaluation

Three performance metrics were used to evaluate the performance of the algorithms with our datasets. Although no consensus on the best performance metric among the numerous existing metrics has been achieved (Botchkarev, 2019), we selected mean absolute percentage error (MAPE) (Eq. (1)) and mean absolute percentage error (RMSPE) (Eq. (2)), which are the respective percentage-error measures of the two most common scale-dependent metrics, mean absolute error and root mean square error (Botchkarev, 2019). R^2 (Eq. (3)) was also used to confirm the linear correlation between the predicted and actual values.

$$\text{MAPE} = \frac{100}{n} \sum_{i=1}^n \left| \frac{\hat{y}_i - y_i}{y_i} \right| \quad (1)$$

$$\text{RMSPE} = \sqrt{\frac{100}{n} \sum_{i=1}^n \left(\frac{\hat{y}_i - y_i}{y_i} \right)^2} \quad (2)$$

$$R^2 = 1 - \frac{\sum_{i=1}^n (\hat{y}_i - y_i)^2}{\sum_{i=1}^n (\bar{y}_i - y_i)^2} \quad (3)$$

where y_i denote the i th observation of objective value y . \hat{y}_i is the i th predicted value of y . Fig. 4 compares the performance of the six different algorithms based on MAPE, where a lower MAPE value indicates better model performance. Half of the observations, which were randomly selected, were used for model construction (training data/in-sample data), and the other half (test data/out-of-sample data) were used for

model evaluation; in-MAPE and out-MAPE denote the MAPEs based on the in-sample and out-of-sample data, respectively.

The lowest average out-MAPE was RF, followed in order by MARS, SVR, GAM, ANN, and OLS. Although most of the algorithms had the flexibility to capture nonlinearities among the variables, the tree-based algorithms (MARS and RF), which can model interactions as well as nonlinearities between variables, showed high predictive performance for out-of-sample data, indicating that the interaction effects among multiple factors on electricity demand cannot be ignored. Although the out-MAPEs for RF were the lowest, it was almost as same as out-MAPEs for MARS. In addition, the in-MAPEs for RF were much lower than the out-MAPEs for RF, whereas there was almost no difference between in-MAPEs and out-MAPEs for MARS. In other words, the estimates of RF showed a high dependence on training data even though it was as robust as MARS. We therefore considered that RF, which is an ensemble learning method based on classification and regression tree (CART), cannot capture the continuity of potential model structure because of its use of piecewise estimates, even though it can build a robust model through its ensemble method that principally avoids overfitting (i.e., reduces variance). These traits raise the concern that TRFs simulated using RF may be affected by features of the training data.

The ascending order of elapsed average running time for a single model construction was OLS, GAM, MARS, SVR, ANN, and RF. MARS had relatively low computational costs in spite of its high predictive performance. In addition, estimates by ANN in some regions were not stable despite model hyperparameters were tuned.

The MAPE evaluation results were confirmed by RMSPE and R^2 (Appendix D). In summary, MARS performed best with our dataset in terms of predictive performance, generalization ability for out-of-sample data, expected smoothness in the TRFs, and computational time.

3.3. Selected algorithm: MARS

A description of MARS and the model building process (Friedman, 1991) is summarized in Appendix E. The contributions of MARS to the proposed methodology are outlined below.

MARS allows us to construct flexible regression models with high-dimensional data. The models are flexible enough to model nonlinearity between variables (i.e., they have a low bias), but they prevent too much flexibility because of the backward pass process incorporated

EPC names	The most populated city in each region		
	City name	LAT North	LONG East
1.Hokkaido	Sapporo	43°04'	141°20'
2.Tohoku	Sendai	38°16'	140°54'
3.Hokuriku	Kanazawa	36°35'	136°38'
4.Tokyo	Tokyo	35°42'	139°45'
5.Chubu	Nagoya	35°10'	136°58'
6.Kansai	Osaka	34°41'	135°31'
7.Chugoku	Hiroshima	34°24'	132°28'
8.Shikoku	Matsuyama	33°51'	132°47'
9.Kyushu	Fukuoka	33°35'	130°23'
10.Okinawa	Naha	26°12'	127°41'

Table 1

Data and candidate variables used in this study.

		Variable name (abbreviation)	Unit	Data description	Data source
Objective variable		Historical electricity demand (EC)	MW	Hourly electricity demand in each electric power company's jurisdictional area	Organization for Cross-regional Coordination of Transmission Operators, 2020
Candidate predictors (explanatory variables)	Meteorological indicators	Temperature (TEMP)	°C	Hourly average air temperature	Japan Meteorological Agency, 2020
		Humidity (HUM)	%	Hourly average relative humidity	
		Solar radiation (SUN)	MJ/m ²	Hourly total solar radiation	
		Wind speed (WIND)	m/s	Average wind speed during the 10 min before each hour	
		Rainfall (RAIN)	mm	Hourly total rainfall	
		Snowfall (SNOW1)	cm	Hourly snowfall since the previous observation time	
		Snow depth (SNOW2)	cm	Hourly depth of the new and old snow remaining on the ground at the observation time	
	Thermal indices	Discomfort index (DI)	-	DI = 0.81 (TEMP) + 0.01 (HUM) (0.99 (TEMP) - 14.3) + 46.3 Also referred to as the temperature-humidity index, represents the human comfort level in summer (Thom, 1959). Equation of Ohashi (2010) are used.	Derived from meteorological indicators
Indicators for human activities		Wind chill index (WCI)	-	WCI = (33 - TEMP) (10.45 + 10 (WIND ^{0.5}) - WIND) WCI represents how cold air feels on human skin and is derived from temperature and wind speed data. Equation of Ohashi (2010) are used.	Calendars in FY2016–FY2018
		Dew point temperature (DPT)	°C	The temperature to which air must be cooled to become saturated with water vapor. Calculated using the function "humidity.to.dewpoint" in R-Package 'weathermetrics' (Anderson et al., 2013).	
		Sundays and holidays dummy (SunD)	-	Sundays and holidays were set to one; all other days were set to zero	
		Saturdays dummy (SatD)	-	Saturdays were set to one; all other days were set to zero	
	Daily routine	Consecutive holidays dummy (ConD)	-	Consecutive holidays such as the New Year and the Bon festival were set to one; all other days were set to zero	NHK Broadcasting Culture Research Institute, 2015
		Non-working day dummy (NwdD)	-	Weekends, holidays, the New Year, and the Bon festival were set to one; all other days were set to zero	
		Working population (WORK%)	%	Percentage of people who are working at the hour	
		Sleeping population (SLEEP%)	%	Percentage of people asleep at the hour	
		Stay home population (HOME%)	%	Percentage of people who are at homes at the hour	
		Awake population (AWAKE%)	%	Percentage of people awake in their homes at the hour	

into the model building process (i.e., low variance). The flexibility and robustness contribute to capturing the nonlinear relation among many factors that determine the level of electricity demand without overfitting. In addition, partially applied linear models based on the hinge functions used in MARS allow capturing a smooth structure of estimates than the piecewise constant segmentation used by recursive partitioning.

MARS also can model the interactions among multiple variables. This trait is indispensable for our method of generating TRFs because electricity modeling often involves interactions among predictors; for example, the effect of the temperature changes depending on the humidity level (Sailor and Muñoz, 1997; Wang and Bielicki, 2018; Hiruta et al., 2019; Maia-Silva et al., 2020).

MARS models are simple to understand and interpret in comparison with other flexible models (e.g., RF, SVM, or ANN). The model can separately present the form that identifies the additive contributions and those associated with the different multivariable interactions. In addition, MARS excludes unimportant variables automatically. Variable selection among multiple correlated variables and the interpretability of the effect of each variable are important for TRF determination because it is related to the sensitivity-detection of electricity demand on a single variable, i.e., temperature.

The MARS algorithm can construct models with large datasets in a fairly short time, making predictions quickly relative to the other flexible algorithms (e.g., SVM). This quick model building allows the use of various types of grid-search-based model tuning and many TRF generation tests. In addition, MARS does not require feature scaling; therefore, estimates are not affected by scaling, such as normalization or standardization.

4. Model construction and evaluation

4.1. Model construction

Using MARS, we constructed comprehensive models to explain electricity demand and generate the TRFs. Model construction was iterated 20 times using half of the observations randomly sampled from observations made during FY2016–FY2018 with replacement (this resampling method is called bootstrapping) to confirm model robustness. The models that performed best according to the performance metrics were chosen as the main model for each region. The models were deemed to be robust, and the difference between the best and worst model was less than 0.02% (MAPE).

The description of the main models constructed is shown in Table 3. The average (minimum–maximum) number of selected predictors was 13.9 (12–15) out of 18. The average number of terms was 64.5 (58–71).

4.2. Accuracy and generalization ability

The performance metrics measuring accuracy and generalization are shown in Table 3. The average (minimum–maximum) MAPEs for the in-sample and out-of-sample results were 3.51% (3.10–3.98%) and 3.55% (3.11–3.99%), respectively. The percentage errors represented by performance metrics were small, and the average difference between the in-sample and out-of-sample results was 0.04% (−0.01–0.09%) in MAPE. The results from the other two performance metrics (RMSPE and R²) confirm the results shown by MAPE. The models explain approximately 93.1% (90.8–96.5%) of variation in hourly electricity demand at a regional scale according to out-R²s. Therefore, the constructed models exhibit high quality with respect to the fit and generalization.

Table 2

The candidate algorithms.

Explanation and implementation settings.		References
Linear regression model, ordinary least squares (OLS)	A multiple linear regression model based on OLS. A second-degree polynomial term was used for temperature to model the nonlinear relation between temperature and electricity demand.	–
Generalized additive model (GAM)	Additive model in which the response variable depends linearly on the smoothing spline function terms for nine variables (TEMP, SUN, DI, WCI, DPT, WORK%, AWAKE%, HOME%, SLEEP%) and nine variables (WIND1, HUM, RAIN, SNOW1, SNOW2, and four dummy variables).	Hastie and Tibshirani, 1990 Wood, 2003 Wood, 2004 Wood et al., 2016 Wood, 2017 ^a Cortes and Vapnik, 1995 Meyer et al., 2020 ^a
Support-vector regression (SVR)	The SVM for regression can solve nonlinear problems by creating a hyperplane in higher dimensions. We used the radial basis function kernel ($\gamma = 9$) and applied 1 for hyperparameter C, which represented the penalty of misclassification from soft-margin hyperplane.	Riedmiller and Braun, 1993 Fritsch et al., 2019 ^a
Artificial neural network (ANN)	Neural network with one hidden layer of 6–9 nodes. The number of nodes was tuned based on a grid-search method. A logistic sigmoid function is used as the activation function.	Breiman, 2001
Random forests (RF)	An ensemble learning method based on CART (Breiman, 1984). We tuned the best combination of hyperparameters B (number of trees to grow) and \bar{P} (number of variables randomly sampled as candidates at each split) using a grid-search method.	Liaw and Wiener, 2002 ^a
Multivariate adaptive regression splines (MARS)	Additive model in which the response variable depends linearly on the weighted sum of the basis functions, which take the form of hinge functions or a product of two or more hinge functions. The maximum degree of interaction was set at three, and the maximum number of model terms before pruning was set at 200 to allow sufficient flexibility. See Appendix E for the detail of MARS.	Friedman, 1991 Milborrow, 2020 ^a Shimokawa et al., 2013 ^a

^a References for the implementation of the algorithm.

The agreement between the observed and predicted hourly electricity demand for selected time periods (August as an example of summer) is shown in Fig. 5. The results for other seasons, winterer (February), spring (May), and fall (November), are shown in Fig. F.1. in Appendix F. The hourly predictions (blue line) agree with the observations (black dots) even during consecutive holidays in all four seasons. Visible disagreements were only observed during several days in mid-August. This time coincides with Bon, a traditional summer vacation season in Japan. These are not national holidays, and days are taken off irregularly, depending on the individual or organization during Bon.

4.3. Year dependency (cross-fiscal year validation)

Because we only had datasets for three fiscal years, we conducted cross-fiscal year validations to confirm that the method is not strongly dependent on the conditions of a certain year but would also be applicable to other years. In this validation, the models trained using the data observed in each of the three fiscal years were tested by observations in each of the three fiscal years in each region. Table 4 shows the cross-fiscal year validation results measured by MAPE. The average (minimum–maximum) deterioration for all models for all regions was 1.06% (0.16–2.26%). Although there are no established criteria to judge whether this deterioration level

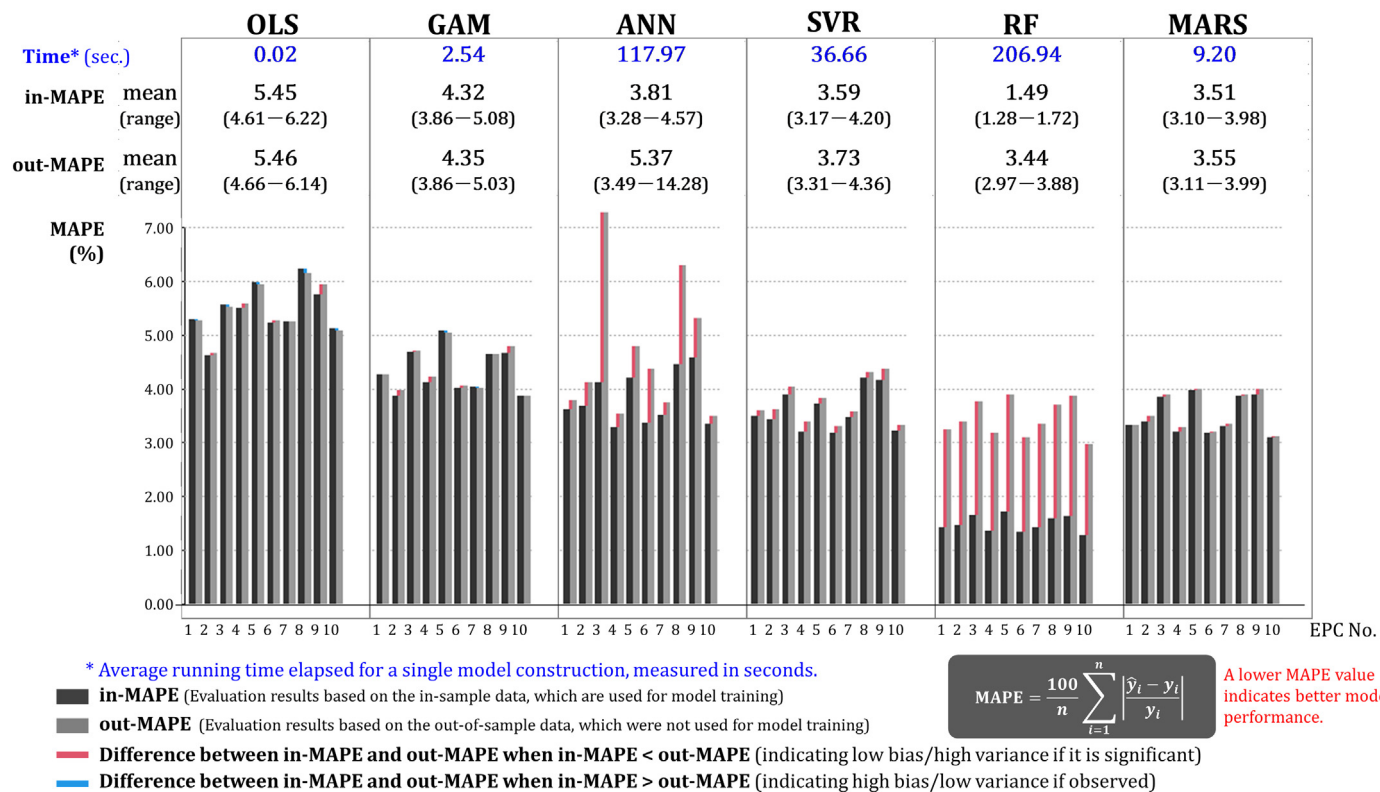


Fig. 4. Performance of six different algorithms evaluated by MAPE (%).

Table 3

Performance and description of the models constructed.

EPCs	Performance metrics						Number of terms	Number of predictors adopted	Number of input predictors			
	MAPE (%)		RMSPE (%)		R2							
	In	Out	In	Out	In	Out						
1. Hokkaido	3.33	3.32	4.32	4.30	0.939	0.938	70	14	18			
2. Tohoku	3.39	3.48	4.47	4.58	0.923	0.917	62	15	18			
3. Hokuriku	3.85	3.88	5.33	5.40	0.915	0.913	71	15	18			
4. Tokyo	3.20	3.27	4.29	4.41	0.953	0.950	62	12	18			
5. Chubu	3.98	3.98	6.04	6.09	0.924	0.923	63	14	18			
6. Kansai	3.17	3.20	4.31	4.32	0.949	0.949	70	15	18			
7. Chugoku	3.30	3.35	4.46	4.49	0.930	0.926	65	14	18			
8. Shikoku	3.87	3.89	5.10	5.11	0.916	0.915	58	13	18			
9. Kyushu	3.89	3.99	5.24	5.40	0.912	0.908	61	14	18			
10. Okinawa	3.10	3.11	4.37	4.20	0.964	0.965	63	13	18			
Average	3.51	3.55	4.79	4.83	0.932	0.931	64.5	13.9	18			
Minimum	3.10	3.11	4.29	4.20	0.912	0.908	58	12	18			
Maximum	3.98	3.99	6.04	6.09	0.964	0.965	71	15	18			

is small enough to guarantee applicability to other years, even in the worst case, the error increased by only 2.26% (when the model for Kyushu was trained by data observed in FY2018 and tested by data observed in FY2016). We infer that the models constructed using our method are not strongly dependent on the conditions of any given year. The results measured by the other performance metrics (RNSPE and R2) shown in Appendix G also support the results by MAPE.

4.4. Contribution of each predictor

Construction of models with high predictive performance, however, is not sufficient; the models must also be of high enough quality to repeatedly

reproduce the sensitivity of electricity demand to temperature under specified conditions. We evaluated the contribution of each predictor in explaining the dispersion in hourly electricity demand based on variable importance (VI) measures. Table 5 lists the VI measures, scaled from 0 to 100, based on the generalized cross validation (GCV) criterion (Craven and Wahba, 1978) for each predictor for each region. These measures examine the difference between GCV for the full model and the model without the information about the targeted predictor; predictors that cause larger net decreases in the GCVs are considered to be more important.

As expected, TEMP had the highest VI of seven meteorological indicators (e.g., Yildiz et al., 2017). Also as expected, SNOW2 exhibited VI only in snowy regions. Although humidity is an important determinant of

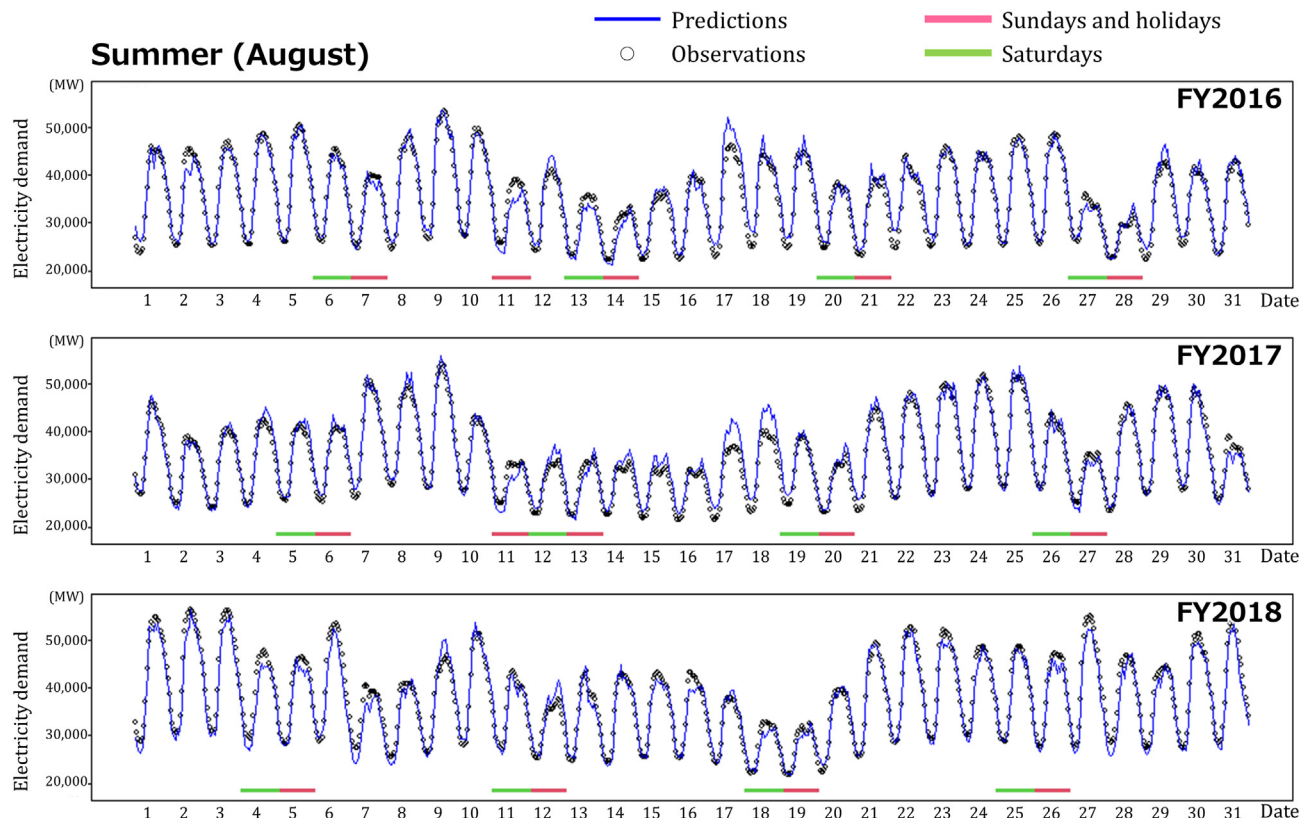


Fig. 5. Observed and predicted hourly electricity demand. The results for Tokyo in summer (August) are shown as examples. The horizontal axis shows the hours in each labeled date of the month, and the vertical axis shows the electricity demand. The hourly predictions (blue line) agree well with the observations (black dots) along the time sequence, even during consecutive holidays. The results for other seasons, winterer (February), spring (May), and fall (November), are shown in Fig. F.1. in Appendix F.

Table 4

Cross-fiscal year validation results (MAPE).

EPC	Test data Training data	MAPE (%)			a. Maximum out-MAPE	b. in-MAPE	Deterioration (a-b)
		FY2016	FY2017	FY2018			
1. Hokkaido	FY2016	2.84	3.83	3.95	3.95	2.84	1.11
	FY2017	3.69	3.05	3.56	3.69	3.05	0.63
	FY2018	4.94	3.65	2.95	4.94	2.95	1.99
2. Tohoku	FY2016	3.15	3.83	3.62	3.83	3.15	0.69
	FY2017	3.60	3.06	3.59	3.60	3.06	0.53
	FY2018	3.67	3.69	3.03	3.69	3.03	0.66
3. Hokuriku	FY2016	3.61	4.56	4.62	4.62	3.61	1.01
	FY2017	4.25	3.40	3.97	4.25	3.40	0.86
	FY2018	4.36	4.04	3.29	4.36	3.29	1.07
4. Tokyo	FY2016	2.86	3.42	4.00	4.00	2.86	1.14
	FY2017	3.38	2.79	3.49	3.49	2.79	0.70
	FY2018	3.77	3.51	2.73	3.77	2.73	1.04
5. Chubu	FY2016	3.59	4.58	5.48	5.48	3.59	1.89
	FY2017	4.16	3.59	4.65	4.65	3.59	1.06
	FY2018	4.80	4.51	3.58	4.80	3.58	1.22
6. Kansai	FY2016	2.86	3.23	3.56	3.56	2.86	0.70
	FY2017	3.27	2.74	3.51	3.51	2.74	0.77
	FY2018	3.58	3.66	2.77	3.66	2.77	0.89
7. Chugoku	FY2016	2.66	3.85	3.91	3.91	2.66	1.25
	FY2017	3.45	2.98	3.72	3.72	2.98	0.74
	FY2018	3.34	4.05	2.92	4.05	2.92	1.13
8. Shikoku	FY2016	3.18	4.07	4.53	4.53	3.18	1.35
	FY2017	3.78	3.41	4.51	4.51	3.41	1.10
	FY2018	4.24	4.75	3.26	4.75	3.26	1.49
9. Kyushu	FY2016	4.22	4.38	4.24	4.38	4.22	0.16
	FY2017	5.01	3.44	4.30	5.01	3.44	1.57
	FY2018	5.29	5.14	3.03	5.29	3.03	2.26
10. Okinawa	FY2016	2.84	3.27	3.74	3.74	2.84	0.90
	FY2017	3.45	2.57	3.31	3.45	2.57	0.88
	FY2018	3.69	3.24	2.68	3.69	2.68	1.01

electricity demand (Sailor and Muñoz, 1997; Wang and Bielicki, 2018; Hiruta et al., 2019; Maia-Silva et al., 2020), HUM was not used in the model. This result is reasonable because DI, which is derived from TEMP and HUM, had a high VI, indicating that DI reflects the demand for cooling resulting from hot, humid conditions better than HUM alone. High VI values for WORK% and SLEEP% also make sense because our daily life cycle affects electricity use. Only Okinawa had relatively low VI values for dummy variables that show the difference in human activity level by date. This result is also reasonable because the main industry in Okinawa is tourism; hence, hotels and other tourist facilities are as active during nonworking days as during working days. In summary, the VI evaluation demonstrated a reasonable contribution of

each predictor in the explanation of the variation in electricity demand in the constructed models.

5. TRF determination

Using the constructed models, we conducted the simulations to determine TRFs while fixing the other variables to specific values to control for the effect of factors other than temperature.

We conducted three types of simulations, S1) hourly simulation to detect hourly segments in TRFs, S2) simulation under the distinct time segments detected by hourly simulation (daytime/nighttime simulation), and S3) monthly simulation to detect seasonal impacts that

Table 5

Variable importance measures for the 10 regions.

Variable name (abbreviation)	1	2	3	4	5	6	7	8	9	10
	Hokkaido	Tohoku	Hokuriku	Tokyo	Chubu	Kansai	Chugoku	Shikoku	Kyushu	Okinawa
Meteorological indicators	TEMP	100	100	100	70	68	62	96	86	79
	HUM	–	–	–	–	–	–	–	–	–
	SUN	42	26	27	29	30	41	33	49	32
	WIND	–	7	19	–	11	4	7	8	13
	RAIN	–	–	–	–	8	4	–	4	20
	SNOW1	–	–	–	–	–	–	–	–	–
	SNOW2	42	10	35	–	–	–	–	–	87
Thermal indices	DI	46	58	96	70	68	47	56	77	63
	WCI	18	15	21	15	–	12	10	–	13
	DPT	17	16	6	4	5	16	13	13	–
Human activities	Difference by date	SunD	34	30	32	31	18	3	48	36
	SatD	11	13	27	12	25	19	22	10	17
	ConD	22	35	47	34	39	36	39	40	34
	NwdD	3	10	58	–	48	26	9	–	19
Daily routine	WORK%	49	81	40	100	100	100	100	32	20
	SLEEP%	36	23	28	58	55	41	56	33	100
	HOME%	42	43	75	29	14	12	11	33	14
	AWAKE%	15	43	35	58	6	14	29	19	25

– denote the variable was not used in the model (VI = 0).

Table 6

Settings for the three types of the simulations conducted.

Name of the simulation		S1) Hourly simulation	S2) Daytime/nighttime simulation	S3) Monthly impact simulation
Purpose of the simulation		To detect hourly segments in TRFs	To acquire distinct TRFs under each hourly segments detected	To detect the seasonal impacts that cannot be explained by meteorological factors
Simulation settings	Predictor(s)	Settings for predictor(s)		
	Meteorological predictor: TEMP	Arithmetic sequence from -10.0°C to 35.0°C at 0.1°C increments		Arithmetic sequence from minimum temperature to maximum temperature in the targeted month at 0.1°C increments
	Meteorological predictors: HUM, SUN, WIND, RAIN, and SNOW2	Fixed at their median values for each time period at each location	Fixed at the median values during daytime hours (10:00–16:00 except 12:00–13:00) at each location	Fixed at the median values during nighttime hours (0:00–4:00) at each location
	SNOW2	Value 0 (indicating no snow accumulation)		
	Thermal indices: DI, WCI, and DPT	Calculated from the meteorological predictors		
	Dummy variables to distinguish day types:	Fixed at a value of 0 to indicate working days		
	SunD, SatD, ConD, and NwdD			
	Daily routine of human activity: WORK%, SLEEP%, HOME%, and AWAKE%	Fixed at the median values for each hour on weekdays	Fixed at the median values during daytime hours (10:00–16:00 except 12:00–13:00) on weekdays	Fixed at the median values during nighttime hours (0:00–4:00) on weekdays
	Monthly dummy variables: Jan, Feb, Mar, Apr, May, Jun, Jul, Sep, Oct, Nov, Dec	Not applied		Fixed at a value of 1 for the targeted month and 0 for the other months.

cannot be explained by meteorological factors. **Table 6** presents settings for the simulations.

5.1. Hourly segments in TRFs

To investigate whether distinct temporal segments in TRFs exist, we simulated TRFs for each hour in 24-h periods using the constructed models. Although we used MARS for main-model construction because of its high performance, the simulation results by other algorithms are also demonstrated to confirm that the general trend of the simulation results is not algorithm-specific. The S1 in **Table 6** presents the settings for hourly simulation (a 24-hour period simulation) for the non-holiday weekdays without snow accumulation.

An arithmetic sequence from -10.0 to 35.0°C at 0.1°C increments was applied for temperature (TEMP). SNOW2 was set as 0 to indicate no snow accumulation. The rest of the meteorological predictors were fixed at their median values for each hour at each location on weekdays. Thermal indices (DI, WCI, DPT) were calculated from the meteorological predictors as shown in **Table 1**. The four dummy variables to distinguish day types (SunD, SatD, ConD, and NwdD) were set as 0 to indicate non-holiday weekdays. The daily routine of human activity predictors (WORK%, SLEEP%, HOME%, and AWAKE%) were set at the values for each hour on weekdays.

Fig. 6a shows the simulated TRFs for each hour in a 24-h period based on the six algorithms, presenting the results for Tokyo as an example. The simulation results (colored lines in **Fig. 6a**) and the observations (dots in **Fig. 6a**) are in good agreement, indicating that the models appropriately reproduced the relationship between temperature and electricity demand. The daytime hours are concentrated on the upper part of each panel, indicating higher demand, whereas the nighttime hours are concentrated in the lower part. These two distinct groups can be recognized regardless of the algorithm used for model building or the region. The results for the rest of the regions are provided in Appendix H.

Fig. 6b shows the value of the normalized BPEs (i.e., the electricity demand value at the bottom of a TRF, **Fig. 1**) for the hourly TRFs of all regions. The BPEs have two distinct levels, one from approximately 9:00 to 20:00 (i.e., during active hours) and the other from approximately 0:00 to 6:00 (i.e., during inactive hours). These periods correspond to the red and blue TRFs in **Fig. 6a**, respectively. Therefore, these two clusters of hours clearly have different electricity demand levels, while the remaining hours are regarded as transition periods between them.

Fig. 6c depicts the BPTs (i.e., the temperature value at the bottom of a TRF, **Fig. 1**) of the hourly TRFs, taking Tokyo as an example. The upper panel in **Fig. 6c** shows the bottom part of the TRFs presented in **Fig. 6a**

(MARS), and the lower panel shows the relation between BPT and the time of day. The BPTs change during the 24-hour period: they average approximately 20°C between 6:00 and 24:00 and approximately 17°C between 0:00 and 6:00. Although the flat section in U-shaped TRFs (i.e., the comfort zone) hinder determination of an explicit BPT and the switch in BPT levels is not clear in some regions (see Appendix I), in general, it is clear that BPTs are different between active hours and inactive hours. Determining explicit BPTs is a topic for further research; a new theoretical model should be developed because there are no explicit thresholds that distinguish V-shaped TRFs and U-shaped TRFs.

Overall, considering the hourly segments detected by the visualized TRFs (**Fig. 6a**), BPEs (**Fig. 6b**), and TRFs (**Fig. 6c**), there are clear time boundaries in the relationship between temperature and electricity demand. Namely, there are two distinct TRFs, one for daytime and one for nighttime.

5.2. Daytime/nighttime simulation

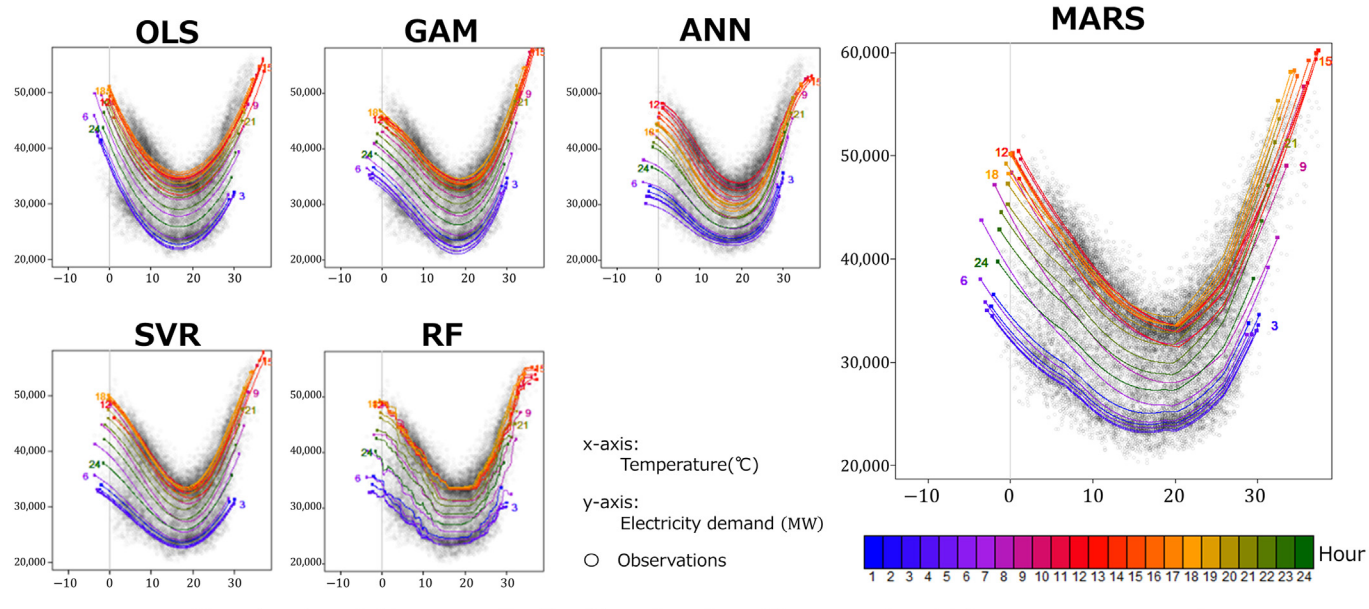
We conducted a simulation to acquire TRFs for daytime and nighttime (see S2 in **Table 6** for the settings of the simulation). In the simulation, to detect the explicit characteristics of the two different TRFs without introducing the variations caused by the gradual transition periods, we used only the core times, i.e., nighttime (0:00–4:00) and daytime (10:00–16:00, except for 12:00–13:00) rather than the entire inactive (0:00–6:00) and active (8:00–24:00) periods. The acquired TRFs for daytime and nighttime are illustrated in **Fig. 7** (dot-lines) and **Fig. 8b**.

5.3. Seasonal segments in TRFs

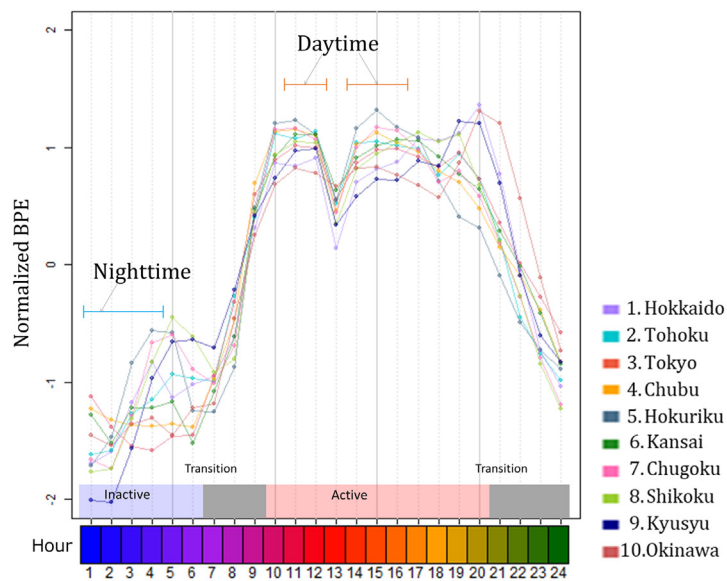
Because seasonal human activities such as events and customs may also affect electricity demand, we constructed models using monthly dummy variables in addition to the predictors listed in **Table 1**.

Table 7 shows the difference in the three performance metrics for out-of-sample results between the models with and without monthly dummy variables; Positive values for out-MAPE (%) and out-RMSPE (%) and negative values for R^2 mean performance improvement due to implementation of monthly dummy variables. The average (minimum–maximum) difference in out-MAPE was 0.24% (0.15% to 0.34%). There were slight improvements in all regions, indicating that small seasonal impacts other than that of meteorological factors do exist, but most of the seasonal impacts are explained by meteorological factors.

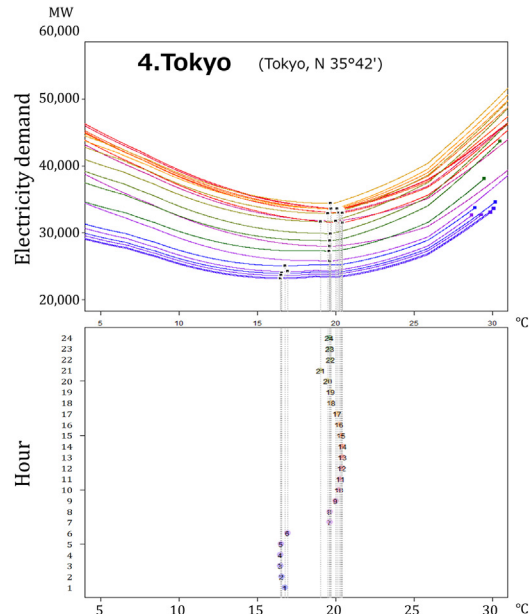
Fig. 7 demonstrates the impacts of the monthly dummy variables (the settings are listed in S3 in **Table 6**), results for Hokkaido, Tokyo, and



a. Hourly simulation results for the six algorithms, using Tokyo as an example.



b. Normalized BPE values for each region in a 24-hour period.



c. BPT values in the hourly TRFs, using Tokyo as an example.

Fig. 6. The results of hourly TRF simulations for the non-holiday weekdays without snow accumulation. (a) Hourly simulation results for the six algorithms, using Tokyo as an example. (b) Normalized BPE values for each region in a 24-hour period. (c) BPT values in the hourly TRFs, using Tokyo as an example. The upper panel shows the bottom part of the TRFs shown in a (MARS), and the lower panel shows the relation between BPT and time of day.

Okinawa are shown as examples. The results for the other regions are illustrated in Fig. J.1 of Appendix J. All settings except for the settings of monthly dummy variables and temperature ranges are the same as those for the daytime/nighttime TRFs (S2). Therefore, the difference between simulation results for daytime and nighttime (S2, dot-line) and the monthly impact simulation result for each month (S3, colored lines) indicate existing seasonal impacts that cannot be explained by meteorological factors.

In northern regions, the differences in TRFs by month are negligible at temperatures around and above BPT, but differences were observed at

low temperatures. The electricity demand tended to be higher during mid-winter months (Dec.–Feb.) than during the seasonal transition months (Oct., Nov., March, and April) at temperatures below BPT. On the other hand, in southern regions such as Okinawa, the differences are observed at higher.

There are small seasonal impacts that cannot be explained by meteorological factors, but they were not as great as two distinct daily temporal differences. Because it is not practical to provide the TRFs for each month or season and the impact is small, we do not consider seasonal impacts other than meteorological impacts to determine regional TRFs.

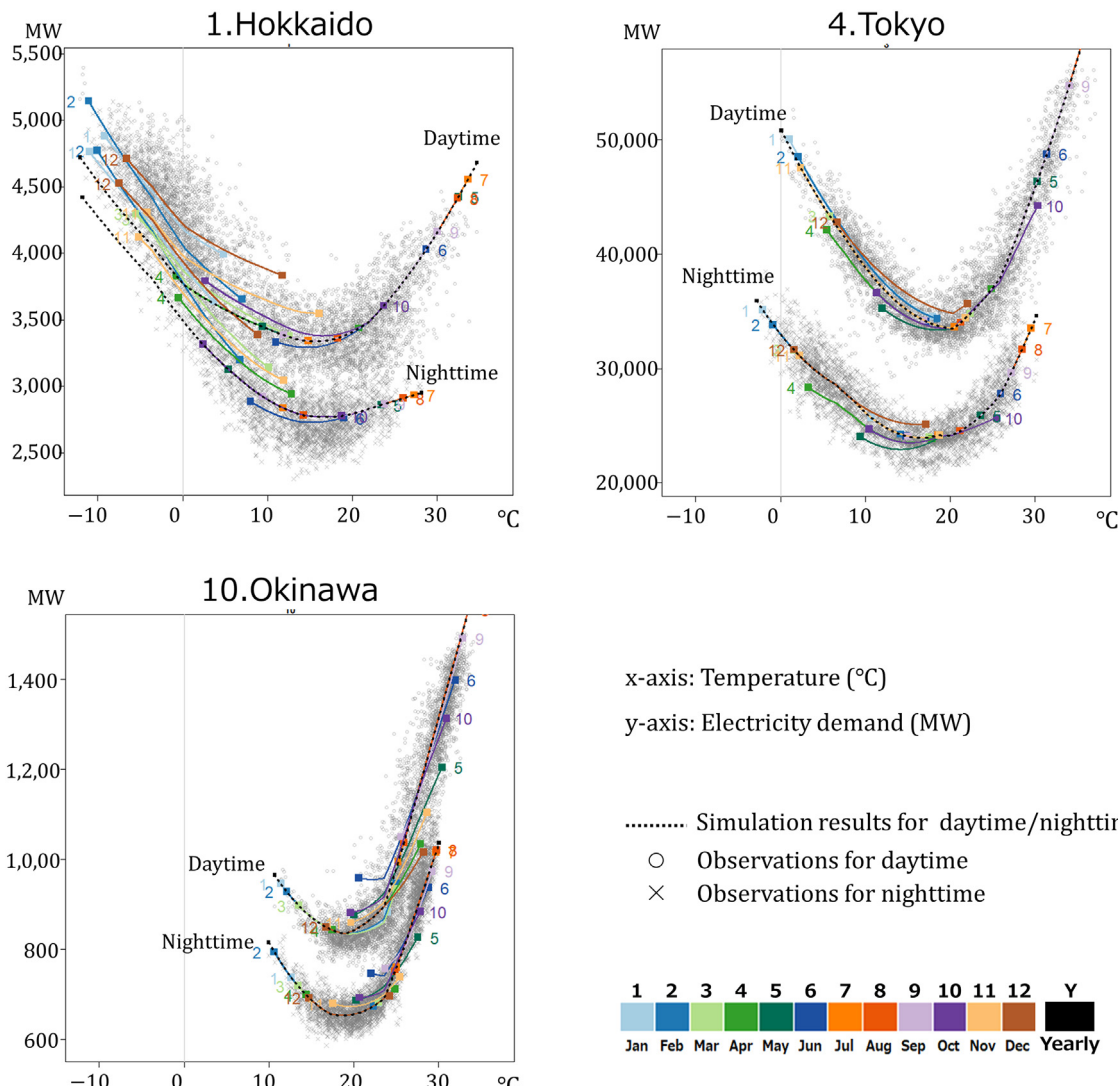


Fig. 7. The results of monthly impact simulation. The simulation settings are listed in S3 in Table 6. The difference between simulation results for daytime and nighttime (S2, dot-line) and the monthly impact simulation result for each month (S3, colored lines) indicate existing seasonal impacts that cannot be explained by meteorological factors. The results for the other regions are illustrated in Fig. J.1 of Appendix J.

5.4. Determination and approximation of TRFs for each region

One of the purposes of obtaining precise TRFs is to apply them in other models, such as impact assessment models. However, the rigorous TRFs obtained in our simulation (daytime and nighttime TRFs, S2) might be too accurate (smooth and flexible) in capturing nonlinearity, and being complex to be applied to other models. Therefore, we approximated the obtained rigorous TRFs by using piecewise linear functions and derived their parameters, such as the coordinates of the breakpoints and coefficients of the regression lines. This approximation was also performed using MARS because the hinges used in the MARS approximation provided simple piecewise functional forms and their parameters. The arithmetic temperature sequence was used as the predictor, and the electricity demand estimated by the derived rigorous TRFs was used as an objective variable for the approximation.

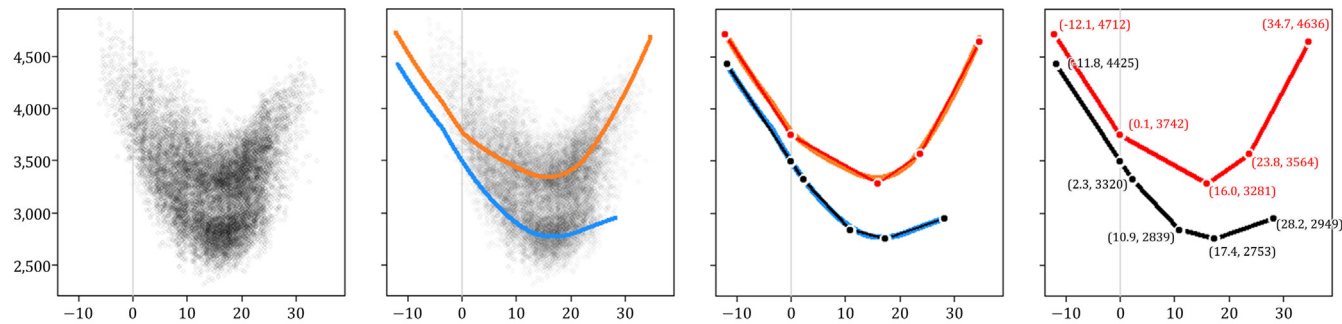
Fig. 8 demonstrates generation and approximation process of TRFs, using Hokkaido, Tokyo, and Okinawa as examples. Fig. 8a shows the observations used to calculate the values for simulation settings. Fig. 8b shows the daytime and nighttime TRFs acquired under the settings S2 in Table 6. The placement of the two simulated TRF lines (orange for daytime

and blue for nighttime) matches the high-density ridges of the corresponding observations (Fig. 8a, b). Fig. 8c, d shows the approximated TRFs superimposed on the simulated TRFs. The piecewise linear approximations appear to appropriately match the simulated rigorous TRFs for both daytime and nighttime. Applied approximation provided piecewise functional forms and their parameters, such as coordinates of the breakpoints and coefficients of the regression lines, listed in Table K.1. of Appendix K. Fig. 8d shows the approximated TRFs with coordinates of the breakpoints. The results are shown for all regions. The results for the other regions are illustrated in Fig. K.1 of Appendix K.

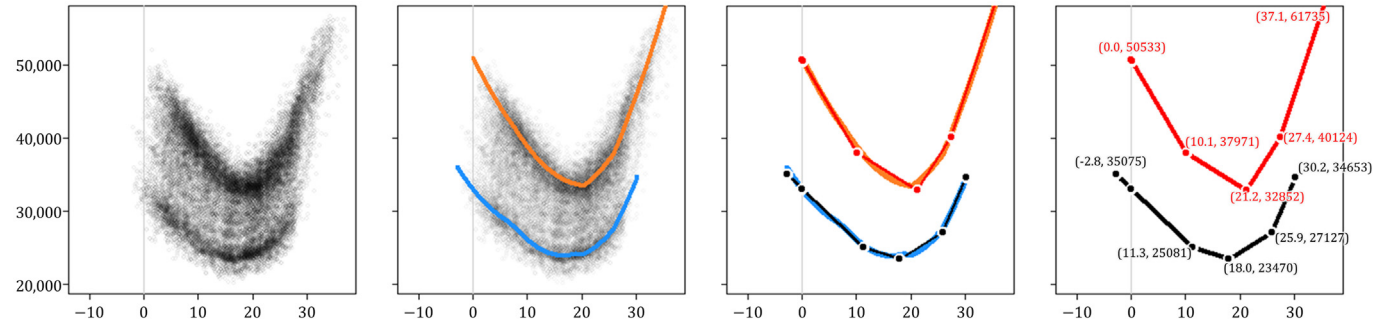
6. Conclusion

We proposed a series of novel methods to generate TRFs at a regional scale and provided reliable TRFs for 10 regions in Japan. We comprehensively modeled the mechanisms through which fluctuations of electricity demand are determined using MARS. Using the constructed models, TRFs for each hour in a 24-h period were generated to detect the time boundaries in the relationship between temperature and electricity demand. We acquired TRFs that represent two distinct time segments detected, one for

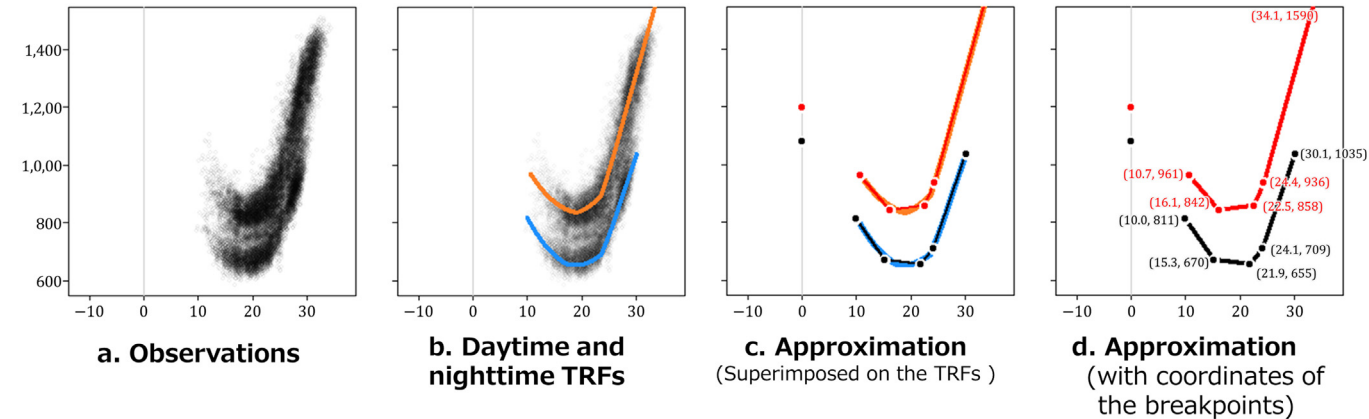
1.Hokkaido (Sapporo, N 43°04')



4.Tokyo (Tokyo, N 35°42')



10.Okinawa (Naha, N 26°12')



x-axis : Temperature (°C)

y-axis : Electricity demand (MW)

○ Observations

b, c — Simulation results for daytime

— Simulation results for nighttime

c, d — Approximations for daytime

— Approximations for nighttime

Fig. 8. Determination and approximation process of TRFs. Observed electricity demand (a). Daytime and nighttime TRFs (b) and their approximations (c), and the coordinates of the breakpoints of the approximations (d). See Appendix K for the results in the rest of the regions. Results for Hokkaido, Tokyo, Kansai, and Okinawa are shown as examples.

daytime and one for nighttime, by conducting additional simulations for each region. We approximated the obtained TRFs by using piecewise linear functions to provide the simple functional forms of TRFs and their parameters. Although the MARS models showed the best performance and generalizability, models based on the other tested algorithms produced similar results. In addition, the model performances were not specific to the conditions of any given year. The outcomes of this research are the proposed methodology, temporal segments in TRFs, and parameters and functional forms.

Three concepts were considered in the development of the proposed method. The first was to construct a comprehensive model that would fully explain the dispersion in hourly electricity demand. For this purpose, we carefully examined the algorithm to be used, the level of the predictive performance and generalization, and the validity of each selected predictor. The MARS was selected as the best algorithm. The contributions of MARS to the proposed methodology are to incorporate nonlinearity and interactions among variables, exclude unimportant variables automatically, and

Table 7

Differences between the model with and without monthly dummy variables assessed by means of three performance metrics.

EPCs	Difference in performance metrics ^a		
	Out-MAPE (%)	Out-RMSPE (%)	Out-R2
1. Hokkaido	0.33	0.42	-0.013
2. Tohoku	0.28	0.38	-0.014
3. Hokuriku	0.21	0.28	-0.010
4. Tokyo	0.22	0.31	-0.007
5. Chubu	0.20	0.23	-0.007
6. Kansai	0.15	0.18	-0.005
7. Chugoku	0.22	0.29	-0.010
8. Shikoku	0.17	0.23	-0.007
9. Kyushu	0.34	0.48	-0.015
10. Okinawa	0.27	0.30	-0.006
Average	0.24	0.31	-0.009
Minimum	0.15	0.18	-0.015
Maximum	0.34	0.48	-0.005

^a (Presented value) = (Performance metric of the model without monthly dummy variables) - (Performance metric of the model with monthly dummy variables); Positive values for out-MAPE (%) and out-RMSPE (%) and negative values for R2 mean performance improvement due to implementation of monthly dummy variables.

construct models with large datasets in a fairly short time. The automatic variable selection contributes to interpretability because the models with an excessive number of predictors can lose interpretability because of the strong correlation among variables, even if the model shows high predictive power. In addition, the application of hourly data is indispensable for the comprehensive modeling considering interactions among variables because the wide dispersion in hourly data provides numerous combinations of determinant factors that occur simultaneously. The second concept was to detect the time boundaries in TRFs for providing rigorous TRFs that represent the relationship between temperature and electricity demand in each region. The third concept was to conduct the simulations to determine TRFs while keeping other variables fixed to control for the effect of factors other than temperature. Only methods based on simulations allow us to generate TRFs under alternative conditions or examine the impacts of specific factors on TRFs. Most previous studies only examined the relation between observed temperature and demand. TRFs acquired by such traditional methods cannot control for the effect of the factors other than temperature, and the parameters obtained from the acquired TRFs are highly dependent on the arbitrariness of the data selected.

Clear temporal divisions were detected in the TRFs; they occurred between the periods when most people are awake (9:00–20:00) and when most people are asleep (0:00–6:00). The divisions differ in regard to both the absolute level of electricity demand and the functional form of the TRFs, including the BPT. Although seasonal impacts other than those related to meteorological factors were detected, they were not as large as that of the usual daily divisions. To the best of our knowledge, this type of finding has not previously been reported.

Finally, we provided TRFs and their parameters for 10 regions of Japan in which the influences of factors other than temperature were fixed, and the complexity of relationships among multiple factors were considered, including nonlinearity, interactions among predictor variables, and temporal segments.

The outcomes of this research, including the proposed methodology, temporal segments in TRFs, and parameters and functional forms, can be used by researchers and decision-makers who are searching for measures to address climate change and UHIs. For example, rigorous TRFs can increase the accuracy of impact assessments of future climate change on electricity demand. This study contributes to decreasing the uncertainty in climate–electricity demand feedback loops, and our method allows for detection of interaction effects, which are necessary for assessing the impacts of anticipated extreme weather events. Rigorous TRFs also provide parameters for analyzing unknown mechanisms of positive feedback loops between increased temperature associated with waste heat from air conditioning and increased demand for air conditioning.

Based on our findings, we recommend the following for the acquisition of accurate TRFs:

- The effects of multiple factors other than temperature must be modeled and controlled to simulate precise TRFs.
- A flexible and stable regression method that considers nonlinearity and interactions should be used for modeling. We currently recommend MARS, although better models should be selected as technology progresses.
- A small number of robust predictors should be selected for implementation in the model, but arbitrary predictor selection should be avoided because it is beyond human ability to select the best predictors among multiple intercorrelated variables.
- Detailed temporal data can provide the necessary dispersion of variables that will contribute to capturing simultaneous interactions among multiple meteorological and human activity factors; they will also increase model performance.
- Finally, temporal segments in the TRFs should be considered when TRFs are applied for multiple analyses, such as in impact assessments of climate change on electricity demand.

We additionally suggest use of direct prediction of electricity demand using constructed regression models whenever possible. This technique is more accurate for assessing the impact that climate change may have on electricity demand compared to the use of TRFs or HDD/CDD. TRFs have been used in existing studies owing to the technical difficulty in the application of complex algorithms in higher-order models and because temperature is the most important meteorological factor and the greatest indicator of climate change. However, the direct implementation of a comprehensive model is becoming a more viable option as the requisite data and sufficient computer power become more widely available.

Some limitations should be noted. As constructed models have a high level of robustness within the training period (FY2016–FY2018) and human physiological responses to thermal environments change little within a span of decades, the TRFs obtained in this study are valid for several years or decades. However, when they are applied to long-term projections, the impacts of factors that change over a longer term, such as socioeconomic factors, human acclimation to warming environment, penetration of air conditioning, resident migration, and technical change in energy demand–supply, also should be considered. Such factors may influence the model parameters as well as the functional form of the TRFs.

The method proposed in this study could be a foundation for future work to incorporate such factors over a longer term. Although long-term training data that include sufficient variation for such factors are not currently available and considerable time will be needed to acquire them, the spatial variation in such factors can be used as an alternative. Future work should be conducted to develop a single nationwide model across regions. Spatial dispersion can be used to estimate model parameters for the factors that change over a longer period in a nationwide model, which could contribute to reducing the uncertainties in future demand projection by applying globally integrated scenario frameworks in which socioeconomic factors are considered.

Socioeconomic changes caused by unprecedented global incidents such as the COVID-19 pandemic can also affect the model parameters and TRFs. The models constructed in this study can contribute to assessing the impact of such incidents on electricity demand by examining the difference between our model predictions and the actual demand during the incident.

Finally, determining explicit BPTs remains as another research topic. Because there are no explicit thresholds that distinguish V-shaped TRFs and U-shaped TRFs, a theoretical model needs to be developed to determine BPT or other indicators that characterize regional TRFs. The TRFs provided in this study can serve as a foundation for such a theoretical model.

CRediT authorship contribution statement

Yuki Hiruta: Conceptualization, Data curation, Formal analysis, Investigation, Methodology, Validation, Visualization, Writing - original draft, and Writing - review & editing. Lu Gao: Writing - review & editing. Shuichi

Ashina: Funding acquisition, Project administration, and Writing - review & editing.

Declaration of competing interest

The authors declare that they have no known competing financial interests or personal relationships
that could have appeared to influence the work reported in this paper.

Acknowledgments

We thank the reviewers and journal editor for their thoughtful comments and efforts towards improving our manuscript. The authors are grateful to NIES members for comments and discussions, to anonymous language editors, and to the funders listed in the funding section.

Funding

This study was supported by the Environment Research and Technology Development Fund (JPMEERF20172011 and JPMEERF20201003) of the Environmental Restoration and Conservation Agency and the Ministry of the Environment, Japan, the Climate Change Adaptation Program of the National Institute for Environmental Studies, Japan, and Grants-in-Aid for Scientific Research JP21K17933 of Japan Society for the Promotion of Science (JSPS).

Data availability

Datasets related to this article can be accessed at the websites hosted by the Organization for Cross-regional Coordination of Transmission Operators of Japan ([Organization for Cross-regional Coordination of Transmission Operators, 2020](#)) and the Japan Meteorological Agency ([Japan Meteorological Agency, 2020](#)), as well as in the report published by NHK Broadcasting Culture Research Institute ([NHK Broadcasting Culture Research Institute, 2015](#)).

Appendix A. Supplementary data

Supplementary data to this article can be found online at <https://doi.org/10.1016/j.scitotenv.2021.152893>.

References

- Allen, M.R., Fernandez, S.J., Fu, J.S., Olama, M.M., 2016. Impacts of climate change on sub-regional electricity demand and distribution in the southern United States. *Nat. Energy* 1, 16103. <https://doi.org/10.1038/nenergy.2016.103>.
- Al-Musaylh, M.S., Deo, R.C., Adamowski, J.F., Li, Y., 2018. Short-term electricity demand forecasting with MARS, SVR and ARIMA models using aggregated demand data in Queensland, Australia. *Adv. Eng. Informatics* 35, 1–16. <https://doi.org/10.1016/j.aei.2017.11.002>.
- Amato, A.D., Ruth, M., Kirshen, P., Horwitz, J., 2005. Regional energy demand responses to climate change: methodology and application to the Commonwealth of Massachusetts. *Clim. Chang.* 71, 175–201. <https://doi.org/10.1007/s10584-005-5931-2>.
- Amber, K.P., Islam, M.W., Hussain, S.K., 2015. Electricity consumption forecasting models for administration buildings of the UK higher education sector. *Energy Build.* 90, 127–136. <https://doi.org/10.1016/j.enbuild.2015.01.008>.
- Anderson, G.B., Bell, M.L., Peng, R.D., 2013. Methods to calculate the heat index as an exposure metric in environmental health research. *Environ. Health Perspect.* 121, 1111–1119.
- Asai, T., Uchida, E., Kawamura, T., 1999. Heibonsha Kisho no Jiten (The meteorological dictionary). Heibonsha Limited, Publishers (In Japanese).
- ASHRAE, 2013. ANSI/ASHRAE Standard 55-2013: Thermal Environmental Conditions for Human Occupancy, ASHRAE standard. ASHRAE (The American Society of Heating Refrigerating and Air-Conditioning Engineers).
- Auffhammer, M., Aroonruengsawat, A., 2011. Simulating the impacts of climate change, prices and population on California's residential electricity consumption. *Clim. Chang.* 109, 191–210. <https://doi.org/10.1007/s10584-011-0299-y>.
- Auffhammer, M., Mansur, E.T., 2014. Measuring climatic impacts on energy consumption: a review of the empirical literature. *Energy Econ.* 46, 522–530. <https://doi.org/10.1016/j.jenecon.2014.04.017>.
- Auffhammer, M., Baylis, P., Hausman, C.H., 2017. Climate change is projected to have severe impacts on the frequency and intensity of peak electricity demand across the United States. *Proc. Natl. Acad. Sci.* 114, 1886–1891. <https://doi.org/10.1073/pnas.1613193114>.
- Beccali, M., Cellura, M., Lo Brano, V., Marvuglia, A., 2008. Short-term prediction of household electricity consumption: assessing weather sensitivity in a Mediterranean area. *Renew. Sust. Energ. Rev.* 12, 2040–2065. <https://doi.org/10.1016/J.RSER.2007.04.010>.
- Bessec, M., Fouquau, J., 2008. The non-linear link between electricity consumption and temperature in Europe: a threshold panel approach. *Energy Econ.* 30, 2705–2721. <https://doi.org/10.1016/j.jenecon.2008.02.003>.
- Botchkarev, A., 2019. A new typology design of performance metrics to measure errors in machine learning regression algorithms. *Interdiscip. J. Information Knowl. Manag.* 14, 045–076. <https://doi.org/10.28945/4184>.
- Braun, M.R., Altan, H., Beck, S.B.M., 2014. Using regression analysis to predict the future energy consumption of a supermarket in the UK. *Appl. Energy* 130, 305–313. <https://doi.org/10.1016/j.apenergy.2014.05.062>.
- Breiman, L., 1984. *Classification and Regression Trees*. Wadsworth International Group.
- Breiman, L., 2001. Random forests. *Mach. Learn.* 45, 5–32. <https://doi.org/10.1023/A:1010933404324>.
- Brown, M.A., Cox, M., Staver, B., Baer, P., 2016. Modeling climate-driven changes in U.S. Buildings energy demand. *Clim. Chang.* 134, 29–44. <https://doi.org/10.1007/s10584-015-1527-7>.
- Christenson, M., Manz, H., Gyalistras, D., 2006. Climate warming impact on degree-days and building energy demand in Switzerland. *Energy Convers. Manag.* 47, 671–686. <https://doi.org/10.1016/J.ENCONMAN.2005.06.009>.
- CIBSE, 2006. *Degree-Days - Theory and Application - TM41*. CIBSE (Chartered Institution of Building Services Engineers).
- Cortes, C., Vapnik, V., 1995. Support-vector networks. *Mach. Learn.* 20, 273–297. <https://doi.org/10.1007/BF00994018>.
- Craven, P., Wahba, G., 1978. Smoothing noisy data with spline functions. *Numer. Math.* 31, 377–403. <https://doi.org/10.1007/BF01404567>.
- De Cian, E., Lanzi, E., Roson, R., 2013. Seasonal temperature variations and energy demand. *Clim. Chang.* 116, 805–825. <https://doi.org/10.1007/s10584-012-0514-5>.
- Dirks, J.A., Gorrisen, W.J., Hathaway, J.H., Skorski, D.C., Scott, M.J., Pulsipher, T.C., Huang, M., Liu, Y., Rice, J.S., 2015. Impacts of climate change on energy consumption and peak demand in buildings: a detailed regional approach. *Energy* 79, 20–32. <https://doi.org/10.1016/j.energy.2014.08.081>.
- Emodi, N.V., Chaiachi, T., Beg, A.B.M.R.A., 2019. The impact of climate variability and change on the energy system: a systematic scoping review. *Sci. Total Environ.* 676, 545–563. <https://doi.org/10.1016/j.scitotenv.2019.04.294>.
- Fazeli, R., Ruth, M., Davidsdottir, B., 2016. Temperature response functions for residential energy demand – a review of models. *Urban Clim.* 15, 45–59. <https://doi.org/10.1016/J.UCLIM.2016.01.001>.
- Fischer, E.M., Knutti, R., 2015. Anthropogenic contribution to global occurrence of heavy-precipitation and high-temperature extremes. *Nat. Clim. Chang.* 5, 560–564. <https://doi.org/10.1038/nclimate2617>.
- Franco, G., Sanstad, A.H., 2008. Climate change and electricity demand in California. *Clim. Chang.* 87, 139–151. <https://doi.org/10.1007/s10584-007-9364-y>.
- Friedman, J.H., 1991. Multivariate adaptive regression splines. *Ann. Stat.* 19, 1–67. <https://doi.org/10.1214/aos/1176347963>.
- Fritsch, S., Guenther, F., Wright, M.N., 2019. *neuralnet: Training of Neural Networks*.
- Hamlet, A.F., Lee, S.-Y., Mickelson, K.E.B., Elsner, M.M., 2010. Effects of projected climate change on energy supply and demand in the Pacific northwest and Washington state. *Clim. Chang.* 102, 103–128. <https://doi.org/10.1007/s10584-010-9857-y>.
- Hashimoto, Y., Ohashi, Y., Nabeshima, M., Shigeta, Y., Kikugawa, Y., Ihara, T., 2019. Sensitivity of electricity consumption to air temperature, air humidity and solar radiation at the city-block scale in Osaka, Japan. *Sustain. Cities Soc.* 45, 38–47. <https://doi.org/10.1016/j.scs.2018.10.004>.
- Hastie, T.J., Tibshirani, R.J., 1990. *Generalized additive models. Monographs on statistics and applied probability*. Chapman and Hall.
- Hirano, Y., Fujita, T., 2012. Evaluation of the impact of the urban heat island on residential and commercial energy consumption in Tokyo. *Energy* 37, 371–383. <https://doi.org/10.1016/j.energy.2011.11.018>.
- Hirano, Y., Gomi, K., Nakamura, S., Yoshida, Y., Narumi, D., Fujita, T., 2017. Analysis of the impact of regional temperature pattern on the energy consumption in the commercial sector in Japan. *Energy Build.* 149, 160–170. <https://doi.org/10.1016/J.ENBUILD.2017.05.054>.
- Hiruta, Y., Gao, L., Ashina, S., 2019. Sensitivity of hourly electricity power consumption to temperature and humidity in Japan (In Japanese). *J. Jpn Soc. Civ. Eng. Ser. G Environ. Res.* 75. https://doi.org/10.2208/jscerer.75.6_II_17-II_27.
- Ihara, T., Genchi, Y., Sato, T., Yamaguchi, K., Endo, Y., 2008. City-block-scale sensitivity of electricity consumption to air temperature and air humidity in business districts of Tokyo, Japan. *Energy* 33, 1634–1645. <https://doi.org/10.1016/j.energy.2008.06.005>.
- Invidiata, A., Ghisi, E., 2016. Impact of climate change on heating and cooling energy demand in houses in Brazil. *Energy Build.* 130, 20–32. <https://doi.org/10.1016/j.enbuild.2016.07.067>.
- Japan Meteorological Agency, 2020. Historical weather data [WWW Document]. <http://www.data.jma.go.jp/obd/stats/etm/index.php>. (Accessed 20 January 2020).
- Kittaka, K., Miyazaki, H., 2014. Temperature sensitivity of power consumption over a wide area (In Japanese). *Archit. Inst. Jpn. J. Environ. Eng.* 79, 891–899. <https://doi.org/10.3130/ajje.79.891>.
- Kiyokawa, Y., Narumi, D., 2018. Regional and secular characteristics on temperature sensitivity of power supply (In Japanese). *J. Environ. Eng.* 83, 1015–1024. <https://doi.org/10.3130/ajje.83.1015>.
- Krese, G., Lampret, Ž., Butala, V., Prek, M., 2018. Determination of a building's balance point temperature as an energy characteristic. *Energy* 165, 1034–1049. <https://doi.org/10.1016/J.ENERGY.2018.10.025>.
- Li, X., Zhou, Y., Yu, S., Jia, G., Li, H., Li, W., 2019. Urban heat island impacts on building energy consumption: a review of approaches and findings. *Energy* 174, 407–419. <https://doi.org/10.1016/j.energy.2019.02.183>.

- Li, Y., Pizer, W.A., Wu, L., 2019. Climate change and residential electricity consumption in the Yangtze River Delta, China. *Proc. Natl. Acad. Sci. U. S. A.* 116, 472–477. <https://doi.org/10.1073/pnas.1804667115>.
- Liaw, A., Wiener, M., 2002. Classification and regression by randomForest. *R News* 2, 18–22.
- Lindelöf, D., 2017. Bayesian estimation of a building's base temperature for the calculation of heating degree-days. *Energy Build.* 134, 154–161. <https://doi.org/10.1016/J.ENBUILD.2016.10.038>.
- Maia-Silva, D., Kumar, R., Nategghi, R., 2020. The critical role of humidity in modeling summer electricity demand across the United States. *Nat. Commun.* 11, 1686. <https://doi.org/10.1038/s41467-020-15393-8>.
- Matzarakis, A., Balafoutis, C., 2004. Heating degree-days over Greece as an index of energy consumption. *Int. J. Climatol.* 24, 1817–1828. <https://doi.org/10.1002/joc.1107>.
- Meyer, D., Dimitriadou, E., Hornik, K., Weingessel, A., Leisch, F., 2020. e1071: Misc Functions of the Department of Statistics, Probability Theory Group (Formerly: E1071), TU Wien.
- Mideksa, T.K., Kallbekken, S., 2010. The impact of climate change on the electricity market: a review. *Energy Policy* 38, 3579–3585. <https://doi.org/10.1016/J.ENPOL.2010.02.035>.
- Milborrow, S., 2020. Earth: multivariate adaptive regression splines [WWW Document]. <https://cran.r-project.org/package=earth>.
- Moazami, A., Nik, V.M., Carlucci, S., Geving, S., 2019. Impacts of future weather data typology on building energy performance – investigating long-term patterns of climate change and extreme weather conditions. *Appl. Energy* 238, 696–720. <https://doi.org/10.1016/j.apenergy.2019.01.085>.
- Morakinyo, T.E., Ren, C., Shi, Y., Lau, K.K.-L., Tong, H.-W., Choy, C.-W., Ng, E., 2019. Estimates of the impact of extreme heat events on cooling energy demand in Hong Kong. *Renew. Energy* 142, 73–84. <https://doi.org/10.1016/j.renene.2019.04.077>.
- Moral-Carcedo, J., Pérez-García, J., 2015. Temperature effects on firms' electricity demand: an analysis of sectorial differences in Spain. *Appl. Energy* 142, 407–425. <https://doi.org/10.1016/J.APENERGY.2014.12.064>.
- Mukherjee, S., Nategghi, R., 2017. Climate sensitivity of end-use electricity consumption in the built environment: an application to the state of Florida, United States. *Energy* 128, 688–700. <https://doi.org/10.1016/j.energy.2017.04.034>.
- Mukherjee, S., Nategghi, R., 2019. A data-driven approach to assessing supply inadequacy risks due to climate-induced shifts in electricity demand. *Risk Anal.* 39, 673–694. <https://doi.org/10.1111/risa.13192>.
- Mukherjee, S., Vineeth, C.R., Nategghi, R., 2019. Evaluating regional climate-electricity demand nexus: a composite Bayesian predictive framework. *Appl. Energy* 235, 1561–1582. <https://doi.org/10.1016/J.APENERGY.2018.10.119>.
- Nategghi, R., Mukherjee, S., 2017. A multi-paradigm framework to assess the impacts of climate change on end-use energy demand. *PLoS One* 12, e0188033. <https://doi.org/10.1371/journal.pone.0188033>.
- NHK Broadcasting Culture Research Institute, 2015. NHK Data Book 2015 National Time Use Survey.
- Nitta, T., Nose, J., Ito, T., Sumi, A., 2005. *Kishō Handobukku (The Handbook of Meteorology)*. Third ed. Asakura Publishing Co., Ltd. (In Japanese).
- Ohashi, Y., 2010. Thermal index (in Japanese). *Tenki* 57, 58–59.
- Organization for Cross-regional Coordination of Transmission Operators J, 2020. Historical energy demand [WWW Document]. <http://occtonet.occto.or.jp/public/dfw/RP11/OCCTO/SD/CC01S042C?fvExtention.pathInfo=CC01S042C&fvExtention.prgbrh=0>. (Accessed 20 February 2020).
- Riedmiller, M., Braun, H., 1993. A direct adaptive method for faster backpropagation learning: the RPROP algorithm. *IEEE International Conference on Neural Networks.*, pp. 586–591.
- Ruth, M., Lin, A.C., 2006. Regional energy demand and adaptations to climate change: methodology and application to the state of Maryland, USA. *Energy Policy* 34, 2820–2833. <https://doi.org/10.1016/j.enpol.2005.04.016>.
- Sailor, D.J., Muñoz, J.R., 1997. Sensitivity of electricity and natural gas consumption to climate in the U.S.A.—methodology and results for eight states. *Energy* 22, 987–998. [https://doi.org/10.1016/S0360-5442\(97\)00034-0](https://doi.org/10.1016/S0360-5442(97)00034-0).
- Schaeffer, R., Szklo, A.S., Pereira de Lucena, A.F., Moreira Cesar Borba, B.S., Pupo Nogueira, L.P., Fleming, F.P., Troccoli, A., Harrison, M., Boulahya, M.S., 2012. Energy sector vulnerability to climate change: a review. *Energy* 38, 1–12. <https://doi.org/10.1016/J.ENERGY.2011.11.056>.
- Segal, M., Shafir, H., Mandel, M., Alpert, P., Balmor, Y., 1992. Climatic-related evaluations of the summer peak-hours' electric load in Israel. *J. Appl. Meteorol.* 31, 1492–1498. [https://doi.org/10.1175/1520-0450\(1992\)031<1492:CREOTS>2.0.CO;2](https://doi.org/10.1175/1520-0450(1992)031<1492:CREOTS>2.0.CO;2).
- Shimokawa, T., Kin, M., Sugimoto, T., Gotō, M., 2013. Tree structured analysis: Jumoku kōzō sekkinhō (in Japanese), R de manabu dēta saiensu, 9. Kyōritsu Shuppan (In Japanese).
- Sigauke, C., Chikobvu, D., 2010. Daily peak electricity load forecasting in South Africa using a multivariate non-parametric regression approach. *ORION* 26. <https://doi.org/10.5784/26-2-89>.
- Thom, E.C., 1959. The discomfort index. *Weatherwise* 12, 57–61. <https://doi.org/10.1080/00431672.1959.9926960>.
- Trust, C., 2012. Degree days for energy management, Tech. rep. [WWW Document]. https://www.sustainabilityexchange.ac.uk/files/degree_days_for_energy_management_carbon_trust.pdf.
- Verbai, Z., Csáky, I., Kalmár, F., 2017. Balance point temperature for heating as a function of glazing orientation and room time constant. *Energy Build.* 135, 1–9. <https://doi.org/10.1016/J.ENBUILD.2016.11.024>.
- Wang, Y., Bielicki, J.M., 2018. Acclimation and the response of hourly electricity loads to meteorological variables. *Energy* 142, 473–485. <https://doi.org/10.1016/j.energy.2017.10.037>.
- Wang, H., Chen, Q., 2014. Impact of climate change heating and cooling energy use in buildings in the United States. *Energy Build.* 82, 428–436. <https://doi.org/10.1016/j.enbuild.2014.07.034>.
- Wang, L., Kubichek, R., Zhou, X., 2018. Adaptive learning based data-driven models for predicting hourly building energy use. *Energy Build.* 159, 454–461. <https://doi.org/10.1016/J.ENBUILD.2017.10.054>.
- Wenz, L., Levermann, A., Auffhammer, M., 2017. North–south polarization of european electricity consumption under future warming. *Proc. Natl. Acad. Sci.* <https://doi.org/10.1073/PNAS.1704339114> 201704339.
- Wood, S.N., 2003. Thin-plate regression splines. *J. R. Stat. Soc. Ser. B Stat. Methodol.* 65, 95–114.
- Wood, S.N., 2004. Stable and efficient multiple smoothing parameter estimation for generalized additive models. *J. Am. Stat. Assoc.* 99, 673–686.
- Wood, S.N., 2017. Generalized Additive Models: An Introduction with R. 2nd ed. Chapman and Hall/CRC <https://doi.org/10.1201/9781315370279>.
- Wood, S.N., Pya, N., S'afken, B., 2016. Smoothing parameter and model selection for general smooth models (with discussion). *J. Am. Stat. Assoc.* 111, 1548–1575.
- Woods, J., Fuller, C., 2014. Estimating base temperatures in econometric models that include degree days. *Energy Econ.* 45, 166–171. <https://doi.org/10.1016/JENEKO.2014.06.006>.
- Yalew, S.G., van Vliet, M.T.H., Gernaat, D.E.H.J., Ludwig, F., Miara, A., Park, C., Byers, E., De Cian, E., Piontek, F., Iyer, G., Mouratiadou, I., Glynn, J., Hejazi, M., Dessens, O., Rochedo, P., Pietzcker, R., Schaeffer, R., Fujimori, S., Dasgupta, S., Mima, S., da Silva, S.R.S., Chaturvedi, V., Vautard, R., van Vuuren, D.P., 2020. Impacts of climate change on energy systems in global and regional scenarios. *Nat. Energy* 5, 794–802. <https://doi.org/10.1038/s41560-020-0664-z>.
- Yıldız, B., Bilbao, J.I., Sproul, A.B., 2017. A review and analysis of regression and machine learning models on commercial building electricity load forecasting. *Renew. Sust. Energ. Rev.* 73, 1104–1122. <https://doi.org/10.1016/J.RSER.2017.02.023>.
- Zhou, Y., Clarke, L., Eom, J., Kyle, P., Patel, P., Kim, S.H., Dirks, J., Jensen, E., Liu, Y., Rice, J., Schmidt, L., Seipley, T., 2014. Modeling the effect of climate change on U.S. State-level buildings energy demands in an integrated assessment framework. *Appl. Energy* 113, 1077–1088. <https://doi.org/10.1016/j.apenergy.2013.08.034>.